ACS Synthetic Biology

Integrating T7 RNA polymerase and its cognate transcriptional units for a host-independent and stable expression system in single plasmid

Xiao Liang, Chenmeng Li, Wenya Wang, and Qiang Li

ACS Synth. Biol., **Just Accepted Manuscript** • DOI: 10.1021/acssynbio.8b00055 • Publication Date (Web): 02 Apr 2018

Integrating T7 RNA polymerase and its cognate transcriptional units for a host-independent and stable expression system in single plasmid

Xiao Liang[a], Chenmeng Li[b], Wenya Wang[b]*, Qiang Li[a]*

[a] Key Laboratory for Industrial Biocatalysis, Ministry of Education, Department of Chemical Engineering, Tsinghua University, Beijing 100084, China

[b] College of Life Science and Technology, Beijing University of Chemical Technology, Beijing 100029, China

*Corresponding authors,

Wenya Wang, Phone: +86-010-64421335

E-mail: wangwy@mail.buct.edu.cn

Qiang Li, Phone: +86-010-62789847

Fax: +86-010-62789847, E-mail: liqiang@tsinghua.edu.cn

Abstract:

Metabolic engineering and synthetic biology usually require universal expression systems for stable and efficient gene expression in various organisms. In this study, a host-independent and stable T7 expression system had been developed by integrating T7 RNA polymerase and its cognate transcriptional units in single plasmid. The expression of T7 RNA polymerase was restricted below its lethal threshold using a T7 RNA polymerase antisense gene cassette, which allowed long-periods cultivation and protein production. In addition, by designing ribosome binding sites, we further tuned the expression capacity of this novel T7 system within a wide range. This host-independent expression system efficiently expressed genes in five different gram-negative strains and one gram-positive strain and was also shown to be applicable in a real industrial D-p-hydroxyphenylglycine production system.

Keywords: Host-independent expression system; Stable expression; Single plasmid; T7 RNA polymerase; antisense RNA

Engineering complex genetic circuits and metabolic pathways in synthetic biology and metabolic engineering has become easier and more efficient with the rapid development of biotechnologies.[1–4] The typical procedure used in synthetic biology and metabolic engineering is to reconstruct metabolic networks in a host by regulating protein expression (or protein activity) or to design a metabolic pathway, resulting in the desired functions or products.[5] Most applications of reconstructed networks are mainly restricted to several model organisms such as *Escherichia coli* and *Saccharomyces cerevisiae*.[6–8] This restriction is due to the limited availability of genetic elements and accessibility of genomic and metabolic data in non-canonical organisms, i.e., their complicated genetic backgrounds.[9,10] However, non-canonical organisms usually have advantages over model organisms; for instance, they naturally produce and tolerate high concentrations of desired products and live in environments with higher or lower pH and temperature values, which are valuable traits for industrial biotechnology.[11,12] Thus, developing some universal genetic elements and circuits, i.e., host-independent systems, for both model and non-canonical organisms is essential and will broaden the choice of hosts applied in synthetic biology and metabolic engineering.[13]

T7 RNAP, originating from bacteriophage T7, has been long studied and widely applied in

engineering genetic circuits and metabolic pathways in roles such as controllers,[14] logic gates,[15] resource allocators,[16] and orthogonal systems.[17] (Fig. S1) Due to its orthogonality, transcriptional efficiency and promoter specificity, T7 RNAP is an excellent candidate for the construction of an ideal host-independent expression system.[18] T7 RNAP functions in a variety of hosts, including prokaryotic, eukaryotic and even cell-free systems.[19–21] The most common way to utilize the T7 expression system relies on a classical approach where it is used by combining DE3 lysogenic hosts (integrating the T7 RNAP gene into the host genome) and cognate plasmids containing T7 promoter-induced transcription units.[19,22] Although the lethal effect of T7 RNAP is attenuated by the reduced amount of T7 RNAP produced from a single copy of the T7 RNAP gene in the genome, the dependence on the preconstruction of DE3 lysogenic hosts limits its universal application in non-canonical hosts.[22] Since the discovery of the T7 system, numerous efforts have been made to construct host-independent T7 expression systems for extending its application to various hosts. However, the majority of these efforts failed due to excessive expression of T7 RNAP, which killed the host cells or caused mutations in the T7 RNAP gene under the biological stress.[23] A few reported successful attempts include the establishment of a two-vector system (low-copy-number and high-copy-number plasmids)[13,24] and the mutation or splitting of T7 RNAP[16,17] to reduce lethal effects and biological stress. Owing to the difficulties in finding two biocompatible plasmids for non-canonical hosts or sacrificing the high transcriptional activity of T7 RNAP, these attempts do not extend the application of the T7 system well. Recently, the work of Manish[13] and Zhao[25] paved a new way for developing T7 expression systems in an extensive range of hosts; although feedback-circuit regulation and gene mining were achieved with T7 systems, the two-vector system and host-dependent system are still used in these studies. These limitations underline the significance to facilitate the development of novel host-independent T7 expression systems through the integration of full-length original T7 RNA polymerase and its cognate transcriptional units into a single plasmid to meet the long-standing request of applying T7 systems as a universal genetic element in various organisms.

Here, we report the implementation of a stable and host-independent expression system containing a T7 RNAP expression cassette and its cognate transcriptional units in single plasmid. The critical idea of our design is to strictly regulate the amount of T7 RNAP produced by a single plasmid system to be below the lethal and biological stress levels. The host-independent

T7 expression system (HITES) efficiently overexpressed heterologous proteins in various gram-positive and gram-negative bacteria, and it was also stable in serial subculture.

Results and Discussion

Operating principle of HITES and instability of the first-generation HITES. Scheme 1 describes the operating principle of HITES designed in this study. The T7 RNAP gene is transcribed into a large number of mRNA molecules under the control of the *lac* promoter (the universality of the *lac* promoter has been evaluated on the basis of the data in Table S1). At the same time, the antisense gene of T7 RNAP in the same plasmid is transcribed into antisense RNA (asRNA) molecules, which can reduce the expression of the T7 RNAP protein by annealing to its cognate mRNA. Consequently, the amount of T7 RNAP will be limited below the lethal threshold, which will guarantee the survival of the host. The limited amount of T7 RNAP can then recognize the T7 promoter on the same plasmid and initiate the transcription of the target gene (*gfp* in this case) at a proper speed. This design allows this HITES to be integrated into any plasmid and work effectively in corresponding hosts.

The construction of the first-generation HITES has been reported in previous work.[26] However, its efficacy was impaired because of its instability during serial subculture (Fig. 1b). The proportion of GFP-free cells increased significantly even after the first subculture, suggesting that the target gene (*gfp*) was not expressed properly in host cells and that the T7 RNAP gene in the HITES might have been mutated; this latter possibility was confirmed by plasmid sequencing. The stability of the first-generation HITES was significantly improved when GLB medium (LB medium contain 1% glucose) was used instead of LB medium (Fig. 1c), but this strategy did not satisfy the laboratory and industrial demands of long serial cultivation.

Construction of a stable inducible HITES. *E. coli* K-12 and *E. coli* B are extensively used in the laboratory and industry. Since *E. coli* JM109 and BL21 are derived from *E. coli* K-12 and B strains, respectively, and both have corresponding DE3 lysogenic hosts, they were selected for testing the expression efficiency and stability of HITES. As shown in Fig. 2a and d, the amount of T7 RNAP in hosts harboring the first-generation HITES (A4A27) was much higher than that in DE3 lysogenic hosts, indicating that the elements in the first-generation HITES were not sufficient to limit the amount of T7 RNAP to non-lethal levels and that a more elaborate regulation of T7 RNAP expression was required for improving the stability of plasmids

harboring a HITES. In the following section, we dissect the contribution of each element, including the asRNA, promoter and terminator, to the amount of T7 RNAP and determine how changes in the T7 RNAP level influenced the expression performance and stability of the HITES.

In the first-generation HITES, a 24 nt long asRNA (A4A27) was used without any supporting sequences, resulting in a low binding capacity and instability for this asRNA.[27,28] In this study, a scaffold sequence for recruiting Hfq protein was added to improve the inhibitory effect of asRNA, yielding the newly designed synthetic asRNA, A4A27-Hfq. Hfq protein enhances the hybridization of asRNA-target mRNA, stabilizes bound asRNA, and facilitates the degradation of target mRNA by recruiting RNases.[29] The introduction of the Hfq binding sequence greatly improved the inhibition of T7RNAP by asRNA in both JM109 (Fig. 2a) and BL21 (Fig. 2d) cells, and the relative fluorescence intensity (RFI) of the GFP slightly increased (Fig. 2b and e). In addition, the GFP fluorescence distribution in BL21 cells was wider than that in JM109 (Fig. 2c and f), this might be due to the differences in the genotype and genetic background of these two strains, leading to the differences in probabilities of plasmid mutation and recombination.[30] However, since the amount of T7 RNAP was still relatively high, additional strategies should be taken to further reduce its level.

The increased stability of the first-generation HITES when GLB medium was used indicated that glucose influenced the activity of the *lac* promoter via the glucose effect.[31] The stability of the HITES could thus be improved by a promoter engineering strategy, which in this case aimed to restrict the activity of the *lac* promoter to a required level. An analysis of *lac* promoter structure revealed two binding sites in the *lac* promoter: the catabolite activator protein (CAP) binding site and the host RNA polymerase binding site, both of which operate coordinately to enhance the expression of *lac* promoter-controlled genes.[32] Mutations or deletion of the CAP binding site could reduce the activity of the *lac* promoter by interfering with the interaction between RNA polymerase and the *lac* promoter.[33] Therefore, the CAP site was deleted from the *lac* promoter that initiated T7 RNAP transcription to generate A4A27-ΔCAP and A4A27-Hfq-ΔCAP. As shown in Fig. 3a, the expression of T7 RNAP was significantly reduced in JM109 cells with a CAP site deletion. The final concentration of T7 RNAP in JM109/A4A27-Hfq-ΔCAP cells (with both synthetic asRNA and a CAP site deletion) was approximately similar to that of JM109(DE3). With the decrease in T7 RNAP expression, the

RFI of cells (Fig. 2b) increased, and the distribution of fluorescent cells (Fig. 2c) significantly improved. Similar results were also obtained in BL21 cells (Fig. 2d, e and f). These results indicated that the synthetic asRNA and CAP site deletion effectively reduced the amount of T7 RNAP below the lethal threshold.

However, when compared with the RFI of DE3 lysogenic hosts, the RFI of A4A27-Hfq-ΔCAP was relatively low (Fig. 2b and e). According to the results above, this difference should not be mainly due to the excessive expression of T7 RNAP. One possible explanation was that the integration of the T7 RNAP gene with its cognate T7 promoter in one plasmid in our system caused the context effects of each component to impair the stability and overall performance of the HITES.[34] Transcriptional read-through by T7 RNAP is a common phenomenon even when the T7 terminator (the termination efficiency was approximately 70%) is used.[35–37] This read-through by T7 RNAP could result in the up-regulation of backbone sequences in the plasmid-based expression system and could hence lead to the abnormal expression of other components on the plasmid.[37] In order to reduce T7 RNAP read-through, we therefore replaced the T7 terminator with a synthetic T7 termination signal (Tz) containing the two transcriptional terminators rrnBT1 and T7, whose termination efficiency is nearly 99% (the final unit with the designed asRNA, CAP site deletion and terminator replacement was denoted the HITES).[37] As shown in Fig. 2b, the RFI of JM109/HITES increased by 76% with the enhancement of termination efficiency and reached a level comparable to that of JM109(DE3). The fluorescent JM109/HITES cells were uniformly distributed with no obvious non-fluorescent cells (Fig. 2c). Similar results were observed in BL21 cells (Fig. 2d, e and f) when they had adopted the HITES. We successfully demonstrated that the performance of the HITES was significantly improved by applying the Tz terminator to overcome read-through transcription of T7 RNAP.

Considering that gene overexpression can cause stress that impairs cell growth, limiting stress to a reasonable level is essential. The stress of the HITES on host growth was thus investigated. (Fig. S2) Our results showed that the growth of JM109/HITES and JM109(DE3) cells did not significantly differ (Fig. S2a). Interestingly, BL21/HITES cells grew better and had higher cell densities than the BL21(DE3) strain (Fig. S2b). On the other hand, since isopropyl β-D-1-thiogalactopyranoside (IPTG) is not suitable for large-scale industrial protein production because of its toxicity and high cost, we used lactose as an expression inducer instead of IPTG;

in this case, the HITES still effectively expressed GFP comparable to DE3 lysogenic hosts (Fig. S3). These results showed that the performance of hosts harboring the HITES were as good as conventional DE3 lysogenic hosts. More importantly, our results demonstrated that T7 expression system could also be applied in a "one-element system"---a single plasmid system, rather than a "two-element system", which contains both a DE3 lysogenic host (that include a chromosomal T7 RNAP) and a plasmid (including a T7 promoter and the target gene).

Stability of the inducible HITES for long-period cultivation. Genetically engineered bacteria need to be continuously subcultured in both laboratory research and industrial production.[9,38] Therefore, the plasmid harboring the HITES must be genetically stable in host cells and not mutate. A serial subculture experiment was carried out to test the stability of the HITES. As shown in Fig. 3a, the RFI fluctuated within a reasonable range, and neither JM109(DE3) nor JM109/HITES cells clearly declined in RFI. Meanwhile, non-fluorescent cells did not appear in Fig. 3b, and the ratio of fluorescent cells remained constant (Fig. 3c). These results underlined the stability of the HITES in *E. coli* JM109 strains.

The stability of the HITES was further tested in *E. coli* BL21 strains. Fig. 4a shows that the RFI of BL21/HITES cells fluctuated within a narrow range. As a positive control, the RFI of BL21(DE3) clearly declined over long periods of serial subculture. Similarly, the distribution of fluorescent cells remained fairly constant in BL21/HITES cells. In contrast, a small number of non-fluorescent cells appeared in BL21(DE3) after the 15th subculture (Fig. 4b), and a clear increase in non-fluorescent cells started. The fluorescence intensities of single cells started to decline significantly in BL21(DE3) cells (Fig. 4b). As shown in Fig. 4c, the ratio of fluorescent BL21/HITES cells stayed higher than this ratio for BL21(DE3) cells after each subculture. This behavior might be because these conventional BL21(DE3) cells were not stable over long periods of cultivation, which was identical to previously reported results.[39,40] This decrease in target gene expression in DE3 hosts was attributed to chromosomal mutations that diminish the level of functional T7 RNA polymerase.[39] In this context, the HITES exhibited better stability in *E. coli* BL21 cells than BL21(DE3) cells, which implied that the expression level of T7 RNAP from the HITES was less toxic in *E. coli* BL21 than the level of T7 RNAP in BL21(DE3) cells. Altogether, the HITES showed an excellent expression capacity and stability by inhibiting the expression of T7 RNAP with optimized asRNA, promoter and terminator engineering. All these results support the hypothesis that limiting the amount of T7 RNAP is the key to successfully

constructing stable HITESs, which provides guidance for other researchers to develop T7 expression systems.

The cross-species application of HITES. To demonstrate that the HITES was able to work efficiently in different host cells, we tested it in three different gram-negative bacteria, including *Pseudomonas putida* KT2440, *Tatumella morbirosei* LMG 23359, *Sinorhizobium* TH572, and one gram-positive bacterium, *Corynebacterium glutamicum* RES167, in addition to *E. coli* JM109 and BL21. *P. putida* and *C. glutamicum* have been widely used in laboratory research and industrial production. *Sinorhizobium* is an important wild-type strain for the industrial production of D-p-hydroxyphenylglycine (D-HPG),[41] while *T. morbirosei* has great potential for replacing the conventional two-step fermentation process in the vitamin C industry with a one-step process.[42] To test the efficacy of the HITES, we first integrated it with a *gfp* reporter gene into a single plasmid that survives in corresponding host and then transformed these plasmids into corresponding host cells separately. Confocal fluorescence microscopy imaging (Fig. 5a) showed that almost all cells exhibited significant GFP fluorescence and that the RFI of hosts harboring the HITES was significantly higher than that of the control (Fig. 5b). These results indicated that the HITES could be universally used in different gram-positive and gram-negative species.

On the other hand, since metabolic engineering often requires multistep enzymatic catalytic reactions for the production of desired chemicals,[38] demonstrating that the HITES can be used to express multiple genes in a multicistron structure in a single plasmid is important. To verify this ability, *lux*AB genes encoding a 41 kDa α subunit and a 37.68 kDa β subunit were selected as reporter proteins. SDS-PAGE (Fig. 5c) showed the high expression levels of *lux*AB genes in *P. putida*, *T. morbirosei*, *C. glutamicum*, and *E. coli*. In summary, the HITES showed excellent performances 1) in different gram-positive and gram-negative strains; 2) in different laboratory and industrial strains; and 3) in single-gene and multi-gene expression systems. These results underlined the potential of using the HITES in different species and multi-gene expression systems for laboratory research and industrial production.

The regulation performance of the HITES. The expression of enzymes involved in a desired pathway must always be finely tuned for an optimized and balanced pathway flux.[9,43] Inclusion bodies consisting of inactive protein aggregates are easily formed using conventional T7 expression systems,[44] and multiple strategies had been adopted to prevent the formation of

inclusion bodies by slowing down the rate of protein synthesis.[45] Here, tuning the amount of T7 RNAP within a wide range was hypothesized to precisely regulate the expression of T7 promoter-cognate genes. The sequence of ribosome binding sites (RBSs) have been shown to strongly affect gene expression at the translational level.[46] Therefore, we designed a series of RBS sequences (Fig. 6b) with different putative T7 RNAP translation rates using the RBS Calculator v2.0 model (Table. S2).[47] As shown in Fig. 6c and d, JM109 and BL21 cells modulated by HITESs containing different RBSs exhibited significant differences in GFP fluorescence, with RFI values ranging from 0.63 to 200.08% and from 0.36 to 149.50%, respectively, relative to the RFI of DE3 lysogenic hosts. This result not only confirmed the strong effect of the RBS sequence on regulating T7 RNAP expression but also provided a good strategy for refining the efficacy of HITES in various hosts to meet the needs of different cases of metabolic engineering, which will be further proven in the following section.

Construction of stable constitutive HITESs in *Sinorhizobium* TH572. The expression of different genes in metabolic networks should vary on a case-by-case basis. For instance, inducible expression is more effective when gene expression is regulated at specific growth stages, whereas for the production of inexpensive products (where the cost of inducer is the main concern), constitutive expression is commonly used for gene expression.[38] *Sinorhizobium* TH572 is an industrial bacterium used to produce D-HPG, which is the precursor of amoxicillin in the bio-pharmaceutical industry.[41] A commonly used method to produce D-HPG depends on an inherent expression system in *Sinorhizobium* TH572 that expresses the enzymes D-hydantoinase (D-Hase) and D-carbamoylase (D-Case) (Fig. 9a). However, the requirement of the toxic, unstable and expensive inducer 5-(2-methylthioethyl)hydantoin made this inherent expression system less practical in industrial production. This limit can be avoided if a constitutive HITES where D-Hase and D-Case are constitutively expressed by T7 RNAP without inducers is used as a substitute. For this purpose, the *lacI* gene, encoding a lactose repressor, was deleted from HITES to realize constitutive gene expression. The deletion of *lacI* caused a sharp decrease in RFI in serial subcultures (Fig. 7a), with non-fluorescent cells appearing and eventually becoming the whole population (Fig. 7b), indicating the instability of the HITES-Δ*lacI* construct. Solving this problem requires reducing the amount of T7 RNAP present.

As described above, the designed RBSs in the former section tuned the T7 RNAP expression level. Five RBSs with lower translation rates (RBS2-6) were selected for constructing

a stable constitutive HITES (Fig. 7c). The results in Fig. 7d indicated that the expression of T7 RNAP decreased corresponding to the putative translation rate of the five RBSs, among which RBS2 caused the strongest reduction. The following subculture experiment demonstrated that RBSs with lower translation rates slowed the fluorescent decay (Fig. 8a-e, left panel) and that the RFI of cells with HITES-RSB2-Δ*lacI* remained steady during long periods of serial subculture (Fig. 8a, left panel). The distribution of fluorescent cells showed the same trend (Fig. 8a-e, right panel), and no clearly non-fluorescent cells were observed when the HITES-RSB2-Δ*lacI* construct was used (Fig. 8a, right panel). Fig. 8f further revealed that the ratio of fluorescent cells was significantly higher when RBSs with lower translation rates were applied. The constitutive expression from HITES-RSB2-Δ*lacI* was stable for at least 20 subculture cycles, which should satisfy the demands of large-scale industrial production, assuming that cells require 27 generations to grow from a 1 milliliter seed culture to a 100 cubic meter culture with the same cell density. In addition, the inoculum volume was 0.1% per subculture in the previous subculture experiment, indicating that the cells grew at a speed of approximately 10 generations per subculture. Thus, the fermentation could theoretically be carried out steadily if the HITES-RSB2-Δ*lacI* construct is stable for at least 3 subcultures, which is far less than 20 subcultures demonstrated above. In conclusion, by using RBSs with different translation rates, the speed of T7 RNAP expression was adjusted to a reasonable level in a given host to achieve stable protein expression.

Constitutive expression of D-Hase and D-Case in *Sinorhizobium* TH572. Based on the results above, the stable, constitutively expressing HITES-RSB2-Δ*lacI* construct was utilized to overexpress D-Hase and D-Case in *Sinorhizobium* TH752. A recombinant strain used in industrial production, *Sinorhizobium*/Hp-C2H, that harbors the inherent inducible promoter was selected as a positive control to investigate the expression capacity of HITES-RSB2-Δ*lacI* in TH752 cells. SDS-PAGE analysis (Fig. 9b) showed that the expression level of D-Hase and D-Case was slightly higher in cells with this construct than in the positive control (*Sinorhizobium*/Hp-C2H). The combined enzyme activity (which was used to evaluate the amount of the active enzymes) of *Sinorhizobium*/Hp-C2H and *Sinorhizobium*/HITES-RBS2-Δ*lacI*-C2H was 1.00U and 1.11U, respectively (Fig. 9c). To conclude, the application of the stable, constitutive HITES in TH572 not only released D-HPG production from the addition of inducer but also exhibited a combined enzyme activity 10.74%

greater than that of the existing industrial strain, demonstrating the industrial value of HITESs in different wild-type strains.

Here, a novel host-independent T7 expression system integrating the T7 RNAP gene and its cognate T7 promoter into the same unit with antisense RNA regulation has been developed. This HITES was integrated into a single plasmid for effective and stable work in host cells, freeing the application of the T7 system from relying on DE3 lysogenic strains. HITES has high transcriptional efficiency, flexible regulation performance and long-lasting genetic stability during subculture. The HITES also worked effectively in one gram-positive and five different gram-negative strains, indicating its universality and powerful application potential in different prokaryotic hosts.

A recent publication reported the Universal Bacterial Expression Resource (UBER), which is an autonomous self-regulated T7 RNAP expression system that functions by combining mixed feedback control loops and cross-species translation signals, and reported it functioning in *E. coli*, *Bacillus subtilis* and *P. putida*.[13] However, there are many advantages of our work comparing to theirs regarding the construction strategy and application fields. First, HITES can be integrated into a single plasmid for stable expression in different hosts, whereas the UBER usually requires two biocompatible plasmids to achieve the efficient expression of target genes, which limits its application in non-canonical hosts. Second, the normal function of the UBER relies on the optimization of both positive and negative feedback loop strengths when applied in a new host, while the expression capacity in our HITES system is effectively tuned by simple RBS engineering. Lastly, unlike the UBER, which is a constitutive expression system with no operon to control target gene expression, we have developed ready-to-use, constitutive HITESs and inducible HITESs for application to different metabolic engineering situations.

Methods

Bacterial strains and culture conditions. *E. coli* JM109, *E. coli* BL21, *P. putida* KT2440, *T. morbirosei* LMG 23359, and *Sinorhizobium* TH572 were cultured in LB broth. *C. glutamicum* RES167 was cultured in LBGU medium (10 g of tryptone, 10 g of NaCl, 5 g of yeast extract, 10 g of glucose and 2 g of urea per liter). Solid media on plates were prepared by adding 1.5% w/v agar. *E. coli* cells were grown at 37°C, *P. putida*, *Sinorhizobium* and *C. glutamicum* were grown

at 30°C, and *T. morbirosei* cells were grown at 28°C. Antibiotic selection for *E. coli* with the single plasmid pET30-HITES was performed with 50 μg/ml kanamycin. Antibiotic selection for *T. morbirosei*, *P. putida* and *Sinorhizobium* with the single plasmid pBBR1MCS5-KT-HITES or pBBR1MCS5-Sino-HITES was performed with 30 μg/ml gentamicin. Antibiotic selection for *C. glutamicum* with the single plasmid pXMJ19-HITES was performed with 12.5 μg/ml chloramphenicol.

Plasmid construction. The coding sequence of synthetic small RNA was synthesized by assembly PCR according to primers designed using DNAWorks (v3.2.4). The various plasmids with CAP deletion, terminator replacement, and designed RBSs were constructed using standard cloning techniques, including PCR, restriction enzyme digestion and ligation. For application in *P. putida* and *T. morbirosei*, a HITES fragment was amplified from pET30-HITES with primers HITES-KT-F and HITES-KT-R, the plasmid fragment was amplified from pBBR1MCS-5 with primers pBBR1MCS5-KT-F and pBBR1MCS5-KT-R, and the HITES fragment was cloned into the plasmid fragment by Gibson assembly, resulting in pBBR1MCS5-KT-HITES. (Fig. S5) For application in *Sinorhizobium*, a HITES fragment was amplified from pET30-HITES with primers HITES-Sino-F and HITES-Sino-R, the plasmid fragment was amplified from pBBR1MCS-5 with primers pBBR1MCS5-Sino-F and pBBR1MCS5-Sino-R, and the HITES fragment was cloned into the plasmid fragment by Gibson assembly, resulting in pBBR1MCS5-Sino-HITES. (Fig. S5) For application in *C. glutamicum*, a HITES fragment was amplified from pET30-HITES with primers HITES-RES-F and HITES-RES-R, the plasmid pXMJ19 was double digested with *Apa* I and *EcoR* I to obtain the plasmid fragment, and the HITES fragment was cloned into the plasmid fragment by Gibson assembly, resulting in pXMJ19-HITES. (Fig. S5) For construction of constitutive HITES, the primers Delete LacI-F and Delete LacI-R were gradient annealed, and the plasmid pBBR1MCS5-Sino-HITES was digested with *Mlu* I/*SgrA* I. The annealed DNA fragment and the digested plasmid were ligated with T4 DNA ligase to generate plasmid pBBR1MCS5-Sino-HITES-Δ*lacI*. The recombinant plasmids were sequenced after their construction. Cloning was conducted in *E. coli* DH5α cells. The sequence of pBBR1MSC-5 and pXMJ19 could be referred to the GenBank accession number U25061.1 and AJ133195.1.

Induction of protein expression. *E. coli* cells were induced with 0.2 mM IPTG at 30°C for 18 hours. *P. putida* and *Sinorhizobium* cells were induced with 0.2 mM IPTG at 30°C for 12 and 24 hours, respectively. *T. morbirosei* cells were induced with 0.2 mM IPTG at 28°C for 18 hours. *C. glutamicum* cells were induced with 0.2 mM IPTG at 30°C for 18 hours. IPTG was added at the beginning of each culture for all inductions.

Fluorescence measurements. To facilitate comparisons of different hosts, the fluorescence intensity was normalized as the fluorescence intensity per OD_{600}. For all the strains used in this study, OD_{600} and fluorescence measurements were recorded using an Infinite M200PRO spectrophotometer (TECAN). Samples were diluted to the proper concentration (OD_{600}=0.3-0.8) before measurement. Samples of 200 μl volumes (triplicate) were transferred to a 96 well transparent microtiter plate for OD_{600} measurements, and a 96 well black microtiter plate for GFP fluorescence measurements. The excitation and emission wavelengths were 485 and 535 nm, respectively. The fluorescence and OD_{600} measurements of the plate wells were conducted after high orbital shaking. Single-cell fluorescence distributions were measured using an S3e Cell Sorter (Bio-Rad). The samples were diluted to 10^6 cells/ml and filtered before injection. The number of collected cells was set to 30,000. In addition, the ratio of fluorescent cells was counted from the results of a flow cytometer.

Growth measurements. Growth curves were recorded using a Bioscreen C (Oy Growth Curves Ab Ltd). Overnight cultures were diluted into LB medium (final volume 300 μl) to a final OD_{600} of 0.05. The incubation temperature was 30°C, and the lid temperature was 31°C. The plate was then cultured with high orbital shaking, and its OD_{600} was measured every 20 min.

Western blot. The OD_{600} values of the cells were measured using an Infinite M200PRO spectrophotometer. Cells with an OD_{600} of 30 were harvested by centrifugation and resuspended to a final volume of 300 μl. Then, 75 μl of 5×SDS-PAGE loading buffer was added to the samples, which were then boiled for 10 min to lyse the cells. The samples were subsequently centrifuged at 13,000 g for 2 min. The supernatant contents were separated by 12% SDS-PAGE under reducing conditions and transferred to a polyvinylidene difluoride (PVDF) membrane (0.45 μm) using 300 mA of current for 2 hours. Membranes were divided into two parts (the

upper part, containing T7 RNAP, and the other part, containing glyceraldehyde 3-phosphate dehydrogenase (GAPDH)) and blocked with 5% skim milk powder in TBST (10 mM Tris-HCl, pH 7.5, 150 mM NaCl, and 0.05% Tween 20) overnight. Membranes were incubated with the indicated antibodies at room temperature for 2 hours. T7 RNAP was incubated with T7 RNAP monoclonal antibody (Novagen, Catalog Number 70566), and GAPDH (selected as reference protein) was incubated with GAPDH rabbit polyclonal antibody (Beijing Biodragon Immunotechnologies Co., Ltd, Catalog Number B1421). The membranes were then washed five times and incubated with peroxidase-conjugated secondary antibody (ZsBio Ltd.). Finally, proteins were detected with High-sig Enhanced Chemiluminescence (ECL) Western Blotting Substrate (Tanon Science & Technology Co., Ltd., Catalog Number 180-501).

Serial subculture experiments. Subculture experiments were carried out according to the procedure shown in Fig. 2a. For *E. coli*, the seed was cultured in LB medium at 37°C for 12 hours, and the culture was then transferred to LB medium with 0.2 mM IPTG at 30°C for 24 hours. For *Sinorhizobium*, the seed was cultured in LB medium at 30°C for 24 hours, and the culture was then transferred to LB medium with 0.2 mM IPTG at 30°C for 24 hours.

Enzyme activity measurement. Recombinant or wild-type *Sinorhizobium* TH572 cells with an OD_{600} of 30 were harvested by centrifugation, and then washed and resuspended in 1/15 M Na_2HPO_4-KH_2PO_4 buffer (pH 8.0) to a final volume of 1 ml. Catalytic reactions were conducted with 9 ml of 0.3% D,L-HPH solution as the substrate at 33°C and 150 rpm for 30 min. Next, 400 μl of 6 M HCl was added to terminate the reaction. The reaction mixture was then centrifuged and cooled in ice.

The concentrations of D-HPG were measured using high-performance liquid chromatography (SHIMADZU, LC-10ATVP). Chromatographic conditions were column: Inertsil ODS-2 packed column (5μm, 4.6×250 mm, Catalog Number 5020-01128); detector: UV-visible detector, 210 nm; flow rate: 1.0 ml/min; mobile phase: water/acetonitrile/phosphoric acid (96:4:0.01, v/v/v). The standard curve of D-HPG standards was constructed under the same chromatographic conditions. In addition, the concentrations of D-HPG in the samples were calculated from the standard curve. The combined enzyme activity was calculated according to the following equation:

$$\text{combined enzyme activity (U/ml)} = \frac{c_S \cdot D_S}{M_D} \cdot \frac{V_2}{V_1 \cdot t}$$

c_S: The concentration of D-HPG in the sample, g/ml

M_D: The molar mass of D-HPG, 167.16 g/mol

D_s: The dilution factor of the sample

V_2: The volume of the reaction mixture, 10 ml in our study

V_1: The volume of the broth diluted in the reaction mixture, 1 ml in our study

t: The reaction time, 30 min in our study

Supporting Information

Supplementary data, including supplementary tables, supplementary figures and database deposition associated with this article can be referenced in the supplementary materials.

Author Information

Corresponding Authors

Qiang Li, *E-mail: liqiang@tsinghua.edu.cn

Wenya Wang, *E-mail: wangwy@mail.buct.edu.cn

Author Contributions

Qiang Li and Wenya Wang conceived this project. Xiao Liang designed and performed all the experiments. Chenmeng Li participated in some of the experiments. Xiao Liang analyzed the data. Xiao Liang, Qiang Li and Wenya Wang wrote the manuscript.

Abbreviations

T7 RNAP, T7 RNA polymerase;

HITES, host-independent T7 expression system;

GFP, green fluorescent protein;

asRNA, antisense RNA;

RFI, relative fluorescence intensity;

RBS, ribosome binding site;

CAP, catabolite activator protein;

IPTG, isopropyl β-D-1-thiogalactopyranoside;

D-HPG, D-p-hydroxyphenylglycine;

D-Hase, D-hydantoinase;

D-Case, D-carbamoylase;

UBER, Universal Bacterial Expression Resource.

Acknowledgment

We thank the National Natural Science Foundation of China (NSFC 21576153) and the Beijing Natural Science Foundation (5162019) for their generous financial support.

References

(1) Lee, S. Y. (2012) Metabolic Engineering and Synthetic Biology in Strain Development. *ACS Synth. Biol. 1*, 491–492.

(2) Pickens, L. B., Tang, Y., and Chooi, Y.-H. (2011) Metabolic Engineering for the Production of Natural Products. *Annu. Rev. Chem. Biomol. Eng. 2*, 211–236.

(3) Cress, B. F., Trantas, E. A., Ververidis, F., Linhardt, R. J., and Koffas, M. A. (2015) Sensitive cells: enabling tools for static and dynamic control of microbial metabolic pathways. *Curr. Opin. Biotechnol. 36*, 205–214.

(4) Bhan, N., Xu, P., and Koffas, M. A. (2013) Pathway and protein engineering approaches to produce novel and commodity small molecules. *Curr. Opin. Biotechnol. 24*, 1137–1143.

(5) Keasling, J. D. (2012) Synthetic biology and the development of tools for metabolic engineering. *Metab. Eng. 14*, 189–195.

(6) Wu, J., Du, G., Zhou, J., and Chen, J. (2013) Metabolic engineering of *Escherichia coli* for (2S)-pinocembrin production from glucose by a modular metabolic strategy. *Metab. Eng. 16*, 48–55.

(7) Yim, H., Haselbeck, R., Niu, W., Pujol-Baxley, C., Burgard, A., Boldt, J., Khandurina, J., Trawick, J. D., Osterhout, R. E., Stephen, R., Estadilla, J., Teisan, S., Schreyer, H. B., Andrae, S., Yang, T. H., Lee, S. Y., Burk, M. J., and Van Dien, S. (2011) Metabolic engineering of *Escherichia coli* for direct production of 1,4-butanediol. *Nat. Chem. Biol. 7*, 445–452.

(8) Runguphan, W., and Keasling, J. D. (2014) Metabolic engineering of *Saccharomyces cerevisiae* for production of fatty acid-derived biofuels and chemicals. *Metab. Eng. 21*, 103–113.

(9) Woolston, B. M., Edgar, S., and Stephanopoulos, G. (2013) Metabolic Engineering: Past and Future. *Annu. Rev. Chem. Biomol. Eng. 4*, 259–288.

(10) Na, D., Kim, T. Y., and Lee, S. Y. (2010) Construction and optimization of synthetic pathways in metabolic engineering. *Curr. Opin. Microbiol. 13*, 363–370.

(11) Paes, B. G., and Almeida, J. R. (2014) Genetic improvement of microorganisms for

applications in biorefineries. *Chem. Biol. Technol. Agric. 1*, 21.
(12) Zeldes, B. M., Keller, M. W., Loder, A. J., Straub, C. T., Adams, M. W. W., and Kelly, R. M. (2015) Extremely thermophilic microorganisms as metabolic engineering platforms for production of fuels and industrial chemicals. *Front. Microbiol. 6*.
(13) Kushwaha, M., and Salis, H. M. (2015) A portable expression resource for engineering cross-species genetic circuits and pathways. *Nat. Commun. 6*, 7832–7843.
(14) Temme, K., Hill, R., Segall-Shapiro, T. H., Moser, F., and Voigt, C. A. (2012) Modular control of multiple pathways using engineered orthogonal T7 polymerases. *Nucleic Acids Res. 40*, 8773–8781.
(15) Shis, D. L., and Bennett, M. R. (2013) Library of synthetic transcriptional AND gates built with split T7 RNA polymerase mutants. *Proc. Natl. Acad. Sci. U. S. A. 110*, 5028–5033.
(16) Segall-Shapiro, T. H., Meyer, A. J., Ellington, A. D., Sontag, E. D., and Voigt, C. A. (2014) A 'resource allocator' for transcription based on a highly fragmented T7 RNA polymerase. *Mol. Syst. Biol. 10*, 742–756.
(17) Meyer, A. J., Ellefson, J. W., and Ellington, A. D. (2015) Directed evolution of a panel of orthogonal T7 RNA polymerase variants for in vivo or in vitro synthetic circuitry. *ACS Synth. Biol. 4*, 1070–1076.
(18) Shis, D. L., and Bennett, M. R. (2014) Synthetic biology: the many facets of T7 RNA polymerase. *Mol. Syst. Biol. 10*, 745–746.
(19) Kortmann, M., Kuhl, V., Klaffl, S., and Bott, M. (2015) A chromosomally encoded T7 RNA polymerase-dependent gene expression system for *Corynebacterium glutamicum*: construction and comparative evaluation at the single-cell level. *Microb. Biotechnol. 8*, 253–265.
(20) Elroy-Stein, O., and Moss, B. (1990) Cytoplasmic expression system based on constitutive synthesis of bacteriophage T7 RNA polymerase in mammalian cells. *Proc. Natl. Acad. Sci. U. S. A. 87*, 6743–6747.
(21) Chizzolini, F., Forlin, M., Cecchi, D., and Mansy, S. S. (2014) Gene Position More Strongly Influences Cell-Free Protein Expression from Operons than T7 Transcriptional Promoter Strength. *ACS Synth. Biol. 3*, 363–371.
(22) Studier, F. W., and Moffatt, B. A. (1986) Use of bacteriophage T7 RNA polymerase to direct selective high-level expression of cloned genes. *J. Mol. Biol. 189*, 113–130.
(23) Davanloo, P., Rosenberg, A. H., Dunn, J. J., and Studier, F. W. (1984) Cloning and expression of the gene for bacteriophage T7 RNA polymerase. *Proc. Natl. Acad. Sci. U. S. A. 81*, 2035–2039.
(24) Gamer, M., Fröde, D., Biedendieck, R., Stammen, S., and Jahn, D. (2009) A T7 RNA polymerase-dependent gene expression system for *Bacillus megaterium*. *Appl. Microbiol. Biotechnol. 82*, 1195–1203.
(25) Zhao, H., Zhang, H. M., Chen, X., Li, T., Wu, Q., Ouyang, Q., and Chen, G.-Q. (2017) Novel T7-like expression systems used for *Halomonas*. *Metab. Eng. 39*, 128–140.
(26) Wang, G., Li, Q., Xu, D., Cui, M., Sun, X., Xu, Y., and Wang, W. (2014) Construction of a host-independent T7 expression system with small RNA regulation. *J. Biotechnol. 189*, 72–75.
(27) Waters, L. S., and Storz, G. (2009) Regulatory RNAs in bacteria. *Cell 136*, 615–628.
(28) Wagner, E. G. H., and Romby, P. (2015) Small RNAs in bacteria and archaea: who they are, what they do, and how they do it, in *Adv. Genet.* (Friedmann, T., Dunlap, J. C., and Goodwin, S. F., Eds.), pp 133–208. Academic Press.
(29) Na, D., Yoo, S. M., Chung, H., Park, H., Park, J. H., and Lee, S. Y. (2013) Metabolic engineering of *Escherichia coli* using synthetic small regulatory RNAs. *Nat. Biotechnol. 31*,

170–174.
(30) Casali, N. (2003) Escherichia coli Host Strains. *Methods Mol. Biol. 235*, 27–48.
(31) Novy, R., and Morris, B. Use of glucose to control basal expression in the pET system. *Novations 13*, 8–10.
(32) Beckwith, J., Grodzicker, T., and Arditti, R. (1972) Evidence for two sites in the *lac* promoter region. *J. Mol. Biol. 69*, 155–160.
(33) Hopkins, J. D. (1974) A new class of promoter mutations in the lactose operon of *Escherichia coli*. *J. Mol. Biol. 87*, 715–724.
(34) Cardinale, S., and Arkin, A. P. (2012) Contextualizing context for synthetic biology – identifying causes of failure of synthetic biological systems. *Biotechnol. J. 7*, 856–866.
(35) Macdonald, L. E., Durbin, R. K., Dunn, J. J., and McAllister, W. T. (1994) Characterization of Two Types of Termination Signal for Bacteriophage T7 RNA Polymerase. *J. Mol. Biol. 238*, 145–158.
(36) Dunn, J. J., Studier, F. W., and Gottesman, M. (1983) Complete nucleotide sequence of bacteriophage T7 DNA and the locations of T7 genetic elements. *J. Mol. Biol. 166*, 477–535.
(37) Mairhofer, J., Wittwer, A., Cserjan-Puschmann, M., and Striedner, G. (2015) Preventing T7 RNA Polymerase Read-through Transcription—A Synthetic Termination Signal Capable of Improving Bioprocess Stability. *ACS Synth. Biol. 4*, 265–273.
(38) Keasling, J. D. (2010) Manufacturing Molecules Through Metabolic Engineering. *Science 330*, 1355–1358.
(39) Vethanayagam, J. G., and Flower, A. M. (2005) Decreased gene expression from T7 promoters may be due to impaired production of active T7 RNA polymerase. *Microb. Cell Factories 4*, 1–7.
(40) Kesik-Brodacka, M., Romanik, A., Mikiewicz-Sygula, D., Plucienniczak, G., and Plucienniczak, A. (2012) A novel system for stable, high-level expression from the T7 promoter. *Microb. Cell Factories 11*, 1–7.
(41) Sheng, W., Liu, Y., Liu, Y., Zhao, G., Wang, J., and Sun, W. (2005) Enzymatic production of D-p-hydroxyphenylglycine from DL-5-p-hydroxyphenylhydantoin by *Sinorhizobium morelens* S-5. *Enzyme Microb. Technol. 36*, 520–526.
(42) Grindley, J. F., Payton, M. A., Pol, H. van de, and Hardy, K. G. (1988) Conversion of Glucose to 2-Keto-l-Gulonate, an Intermediate in l-Ascorbate Synthesis, by a Recombinant Strain of *Erwinia citreus*. *Appl. Environ. Microbiol. 54*, 1770–1775.
(43) Englaender, J. A., Jones, J. A., Cress, B. F., Kuhlman, T. E., Linhardt, R. J., and Koffas, M. A. G. (2017) Effect of Genomic Integration Location on Heterologous Protein Expression and Metabolic Engineering in *E. coli*. *ACS Synth. Biol. 6*, 710–720.
(44) Schumann, W., and Ferreira, L. C. S. (2004) Production of recombinant proteins in *Escherichia coli*. *Genet. Mol. Biol. 27*, 442–453.
(45) Rosano, G. L., and Ceccarelli, E. A. (2014) Recombinant protein expression in *Escherichia coli*: advances and challenges. *Front. Microbiol. 5*, 172.
(46) Salis, H. M., Mirsky, E. A., and Voigt, C. A. (2009) Automated design of synthetic ribosome binding sites to control protein expression. *Nat. Biotechnol. 27*, 946–950.
(47) Tian, T., and Salis, H. M. (2015) A predictive biophysical model of translational coupling to coordinate and control protein expression in bacterial operons. *Nucleic Acids Res. 43*, 7137–7151.

Figure Legends

Scheme 1. The operating principle of the HITES designed in this study. CAP: the CAP binding site of the *lac* promoter, TT: terminator. Elements marked in red fonts were engineered in the following section to generate a stable HITES.

Figure 1. Instability of the first-generation HITES. (a) Schematic representation of the subculture experiment. (b) The fluorescent cell distribution after each subculture in LB medium. (c) The fluorescent cell distribution after each subculture in GLB medium (LB medium containing 1% glucose).

Figure 2. Construction and verification of a stable HITES. (a) The amount of T7 RNAP in JM109 host cells with different modifications (asRNA sequence, CAP deletion, and terminator replacement) was analyzed by western blot using monoclonal antibodies against T7 RNAP. JM109: JM109 harboring pET30-GFP, negative control; JM109(DE3): JM109(DE3) harboring pET30-GFP, positive control; JM109/A4A27: JM109 harboring the first-generation HITES; JM109/A4A27-Hfq: JM109 harboring a HITES with synthetic asRNA; JM109/A4A27-ΔCAP: JM109 harboring a HITES with CAP deletion; JM109/A4A27-Hfq-ΔCAP: JM109 harboring a HITES with synthetic asRNA and CAP deletion; JM109/HITES: JM109 harboring a HITES with synthetic asRNA, CAP deletion and terminator replacement. (b) The RFI of JM109 host cells with different modifications (asRNA sequence, CAP deletion, and terminator replacement). (c) Single-cell GFP fluorescence distributions of JM109 host cells with different modifications (asRNA sequence, CAP deletion, and terminator replacement). (d) The amount of T7 RNAP in BL21 host cells with different modifications (asRNA sequence, CAP deletion, and terminator replacement) was analyzed by western blot using monoclonal antibodies against T7 RNA polymerase. (e) The RFI of BL21 host cells with different modifications (asRNA sequence, CAP deletion, and terminator replacement). (f) Single-cell GFP fluorescence distributions of BL21 host cells with different modifications (asRNA sequence, CAP deletion, and terminator replacement).

Figure 3. Stability of the HITES in *E. coli* JM109 during long periods of serial subculture. (a) The fluorescence intensity changes in JM109(DE3) and JM109/HITES cells measured by

spectrophotometer after each subculture. (b) Single-cell GFP fluorescence distributions of JM109(DE3) and JM109/HITES cells measured by flow cytometer. The numbers 1, 5, 10, 15, 20, and 22 represent the first, fifth, tenth, fifteenth, twentieth, and twenty-second subculture, respectively. (c) The ratio of fluorescent JM109(DE3) and JM109/HITES cells after each subculture, which was determined from the results of a flow cytometer.

Figure 4. Stability of the HITES in *E. coli* BL21 during long periods of serial subculture. (a) The fluorescence intensity changes of BL21(DE3) and BL21/HITES cells measured by spectrophotometer after each subculture. (b) Single-cell GFP fluorescence distributions of BL21(DE3) and BL21/HITES cells measured by flow cytometer. The numbers 1, 5, 10, 15, 20, and 22 represent the first, fifth, tenth, fifteenth, twentieth, and twenty-second subculture, respectively. (c) Ratio of fluorescent BL21(DE3) and BL21/HITES cells after each subculture, which was determined using a flow cytometer.

Figure 5. Universality of the HITES in different gram-positive and gram-negative bacteria. (a) Confocal fluorescence micrograph analysis showing GFP fluorescence in different host cells. The merged images of the confocal fluorescence micrographs and the differential interference contrast (DIC) micrographs are shown. Scale bars, 2 μm. (b) GFP fluorescence intensity of different host cells measured by spectrophotometer. (c) SDS-PAGE analysis of luxAB expression in *P. putida*, *T. morbirosei*, *C. glutamicum*, *E. coli* JM109 and BL21 cells.

Figure 6. The regulation performance of HITESs with different T7 RNAP translation rates. (a) Schematic diagram of how the RBS of T7 RNAP gene could affect its expression in HITESs. (b) Putative translation initiation rate of the designed RBSs according to the RBS Calculator v2.0 model. (c) GFP fluorescence intensity of JM109 cells harboring HITESs with different RBSs measured by spectrophotometer. (d) GFP fluorescence intensity of BL21 cells harboring HITESs with different RBSs measured by spectrophotometer.

Figure 7. Construction of a stable, constitutive HITES in *Sinorhizobium* TH572. (a) The fluorescence intensity changes of *Sinorhizobium*/HITES-ΔlacI measured by spectrophotometer after each subculture. (b) Single-cell GFP fluorescence distributions of

Sinorhizobium/HITES-ΔlacI cells measured by flow cytometer. The numbers 1, 2, 3, 4, 5, and 8 represent the first, second, third, fourth, fifth, and eighth subculture, respectively. (c) Putative translation initiation rate of the designed RBSs according to the RBS Calculator v2.0 model. (d) The amount of T7 RNAP in *Sinorhizobium* harboring constitutive HITESs with different RBSs was analyzed by western blot using monoclonal antibodies against T7 RNAP.

Figure 8. The stability of constitutive HITESs with different RBSs. (a-e) Left: The fluorescence intensity changes of *Sinorhizobium* cells harboring constitutive HITESs with RBS2, RBS3, RBS4, RBS5, and RBS6, respectively. Right: Single-cell GFP fluorescence distributions of *Sinorhizobium* harboring constitutive HITESs with RBS2, RBS3, RBS4, RBS5, and RBS6, respectively. Numbers on the graph represent the iteration number of the subculture. (f) Ratio of fluorescent *Sinorhizobium* cells harboring constitutive HITES with different RBSs after each subculture as counted by a flow cytometer.

Figure 9. Constitutive expression of D-Hase and D-Case in *Sinorhizobium* TH572. (a) Schematic diagram of D-HPG production via the catalysis of two sequentially acting enzymes, D-Hase and D-Case. (b) SDS-PAGE analysis of D-Hase and D-Case expression in wild-type *Sinorhizobium* (negative control), *Sinorhizobium*/Hp-C2H (positive control), and *Sinorhizobium*/HITES-RBS2-ΔlacI-C2H cells. (c) Combined enzyme activity of the corresponding strains measured by HPLC.

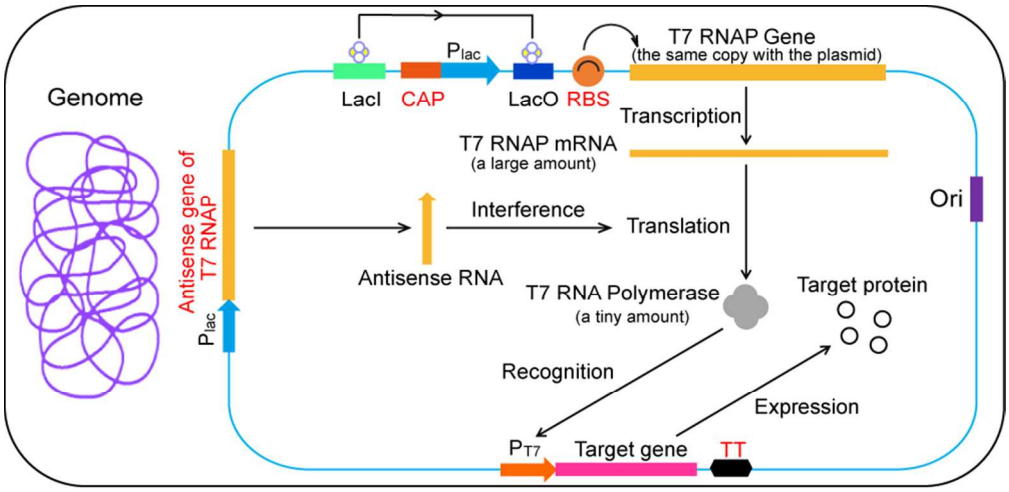

84x40mm (300 x 300 DPI)

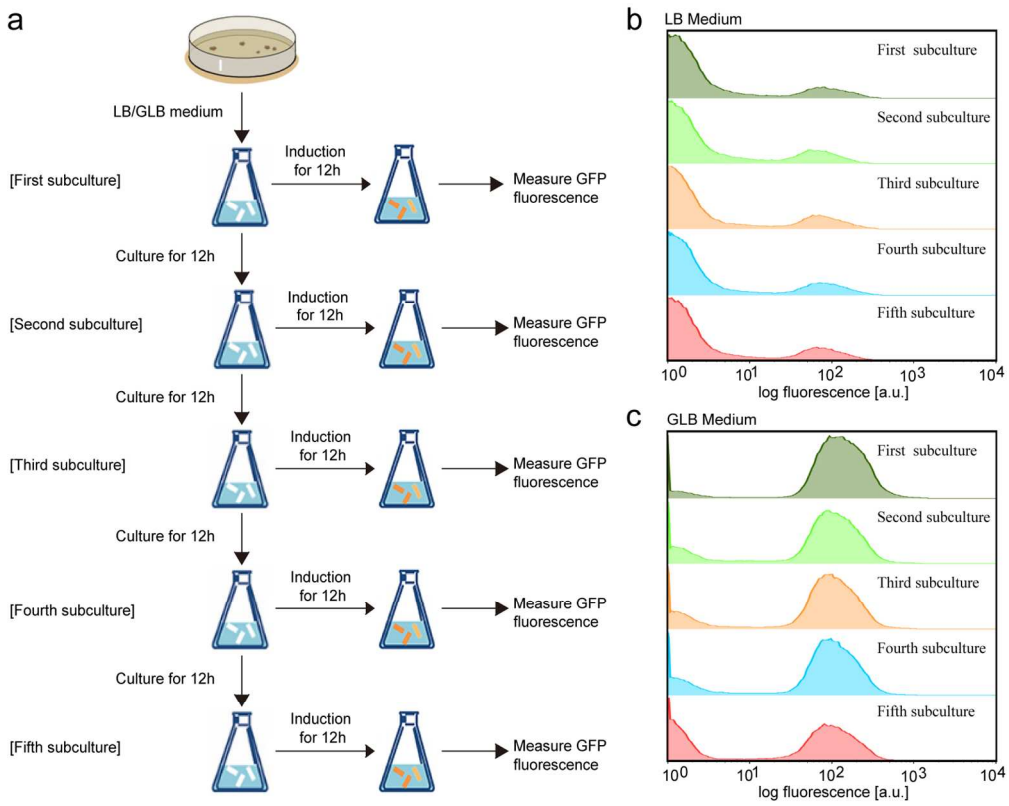

137x109mm (300 x 300 DPI)

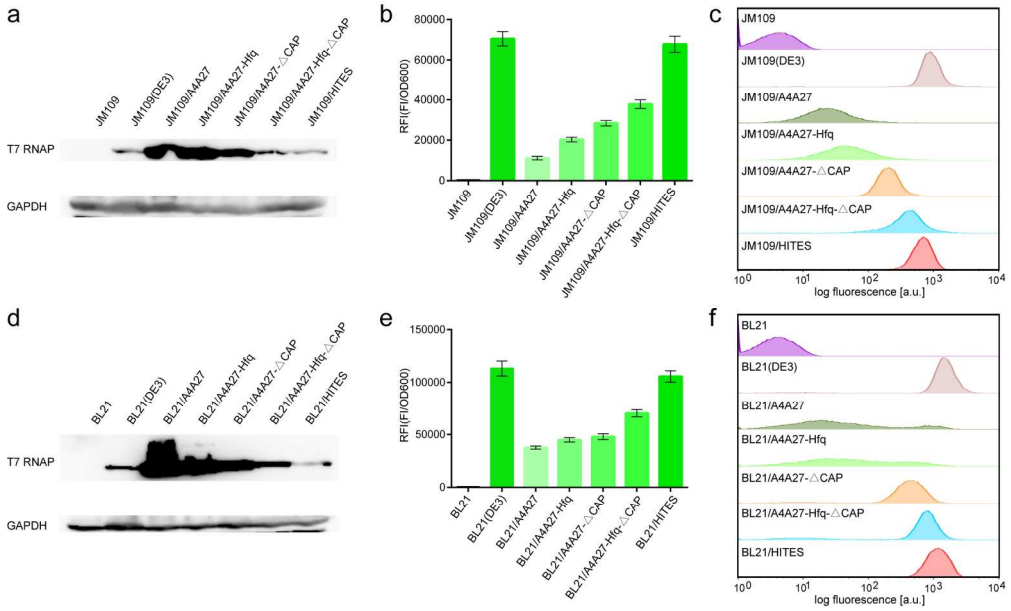

171x105mm (300 x 300 DPI)

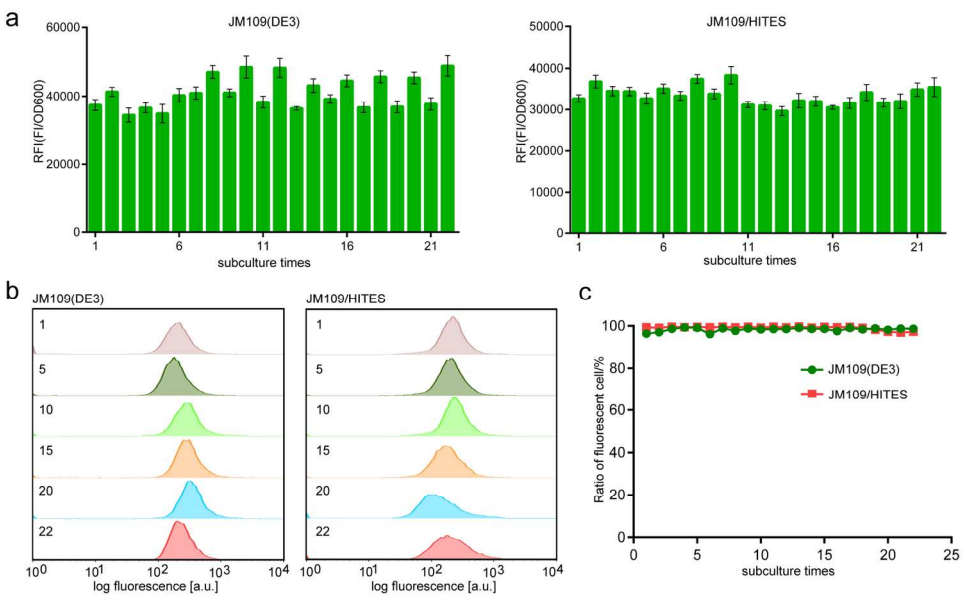

165x98mm (300 x 300 DPI)

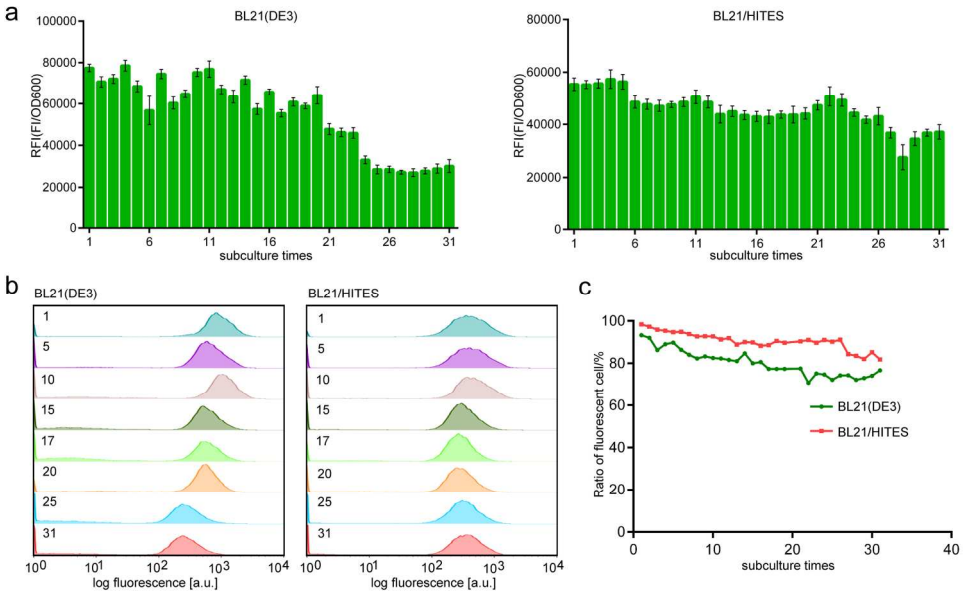

165x98mm (300 x 300 DPI)

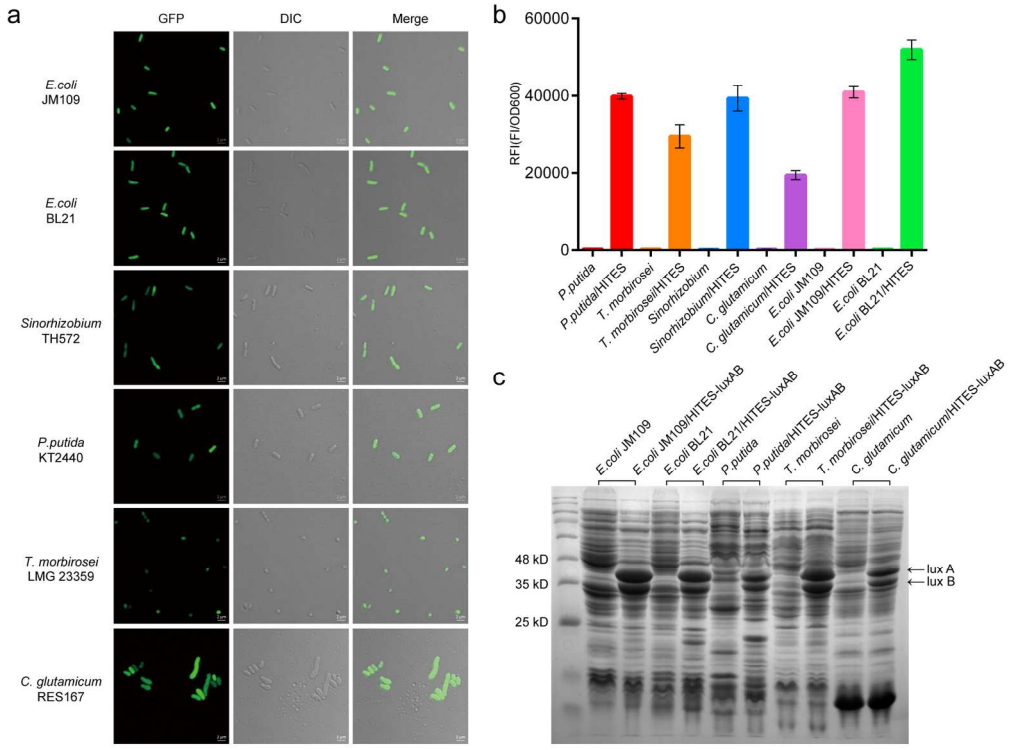

166x128mm (300 x 300 DPI)

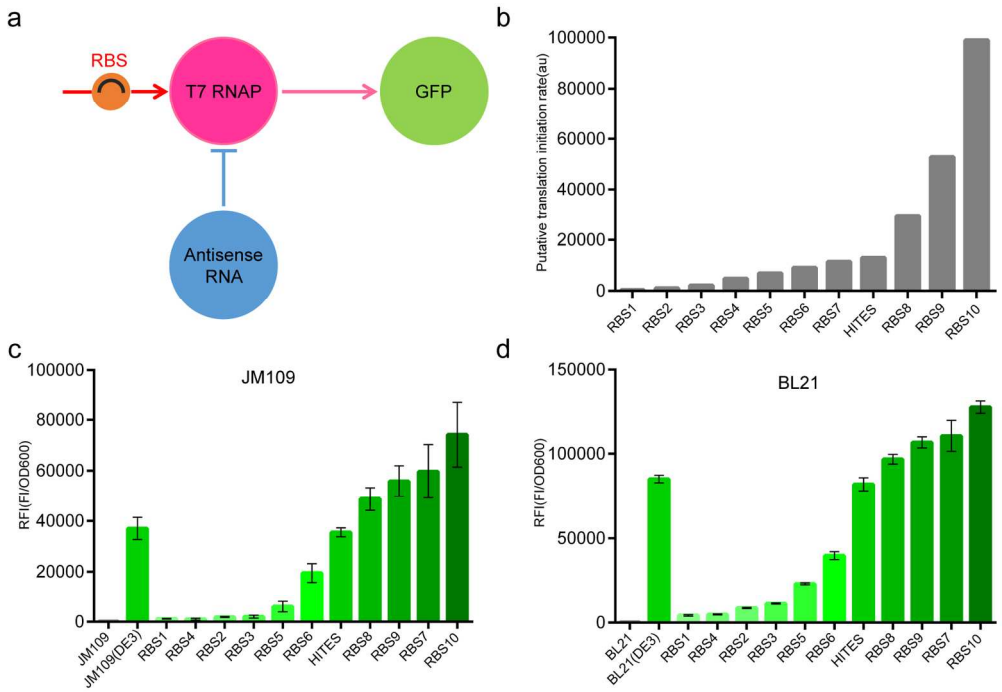

157x108mm (300 x 300 DPI)

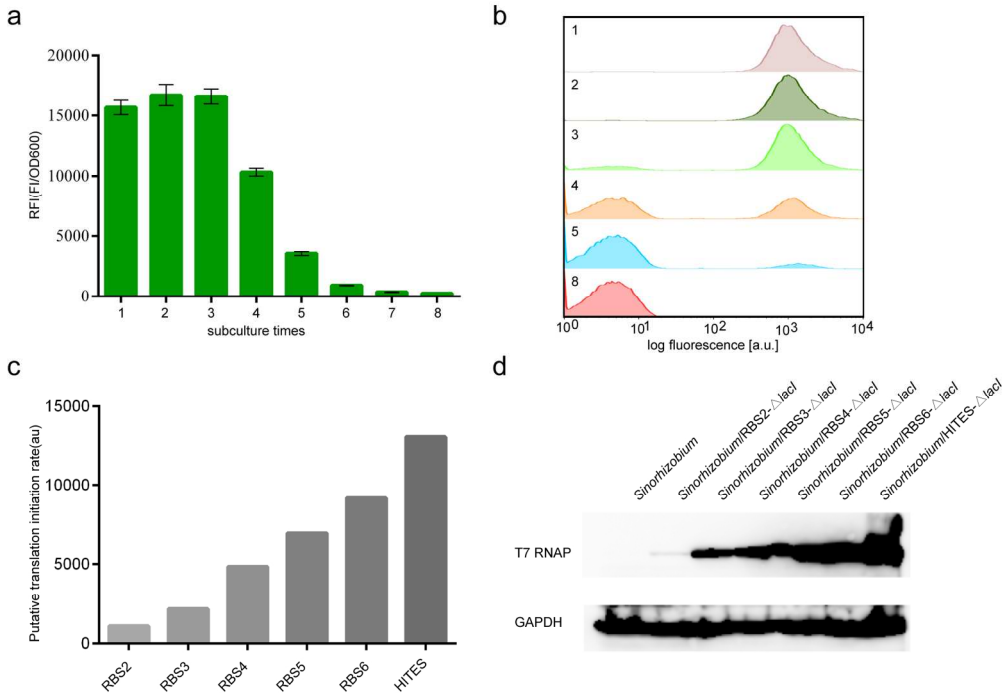

157x110mm (300 x 300 DPI)

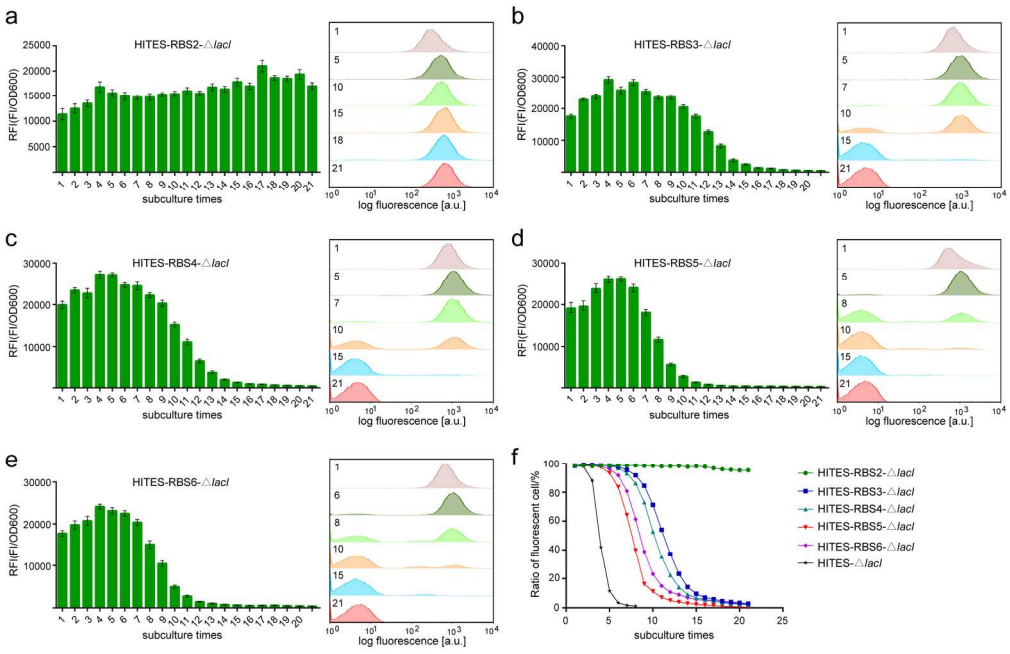

176x114mm (300 x 300 DPI)

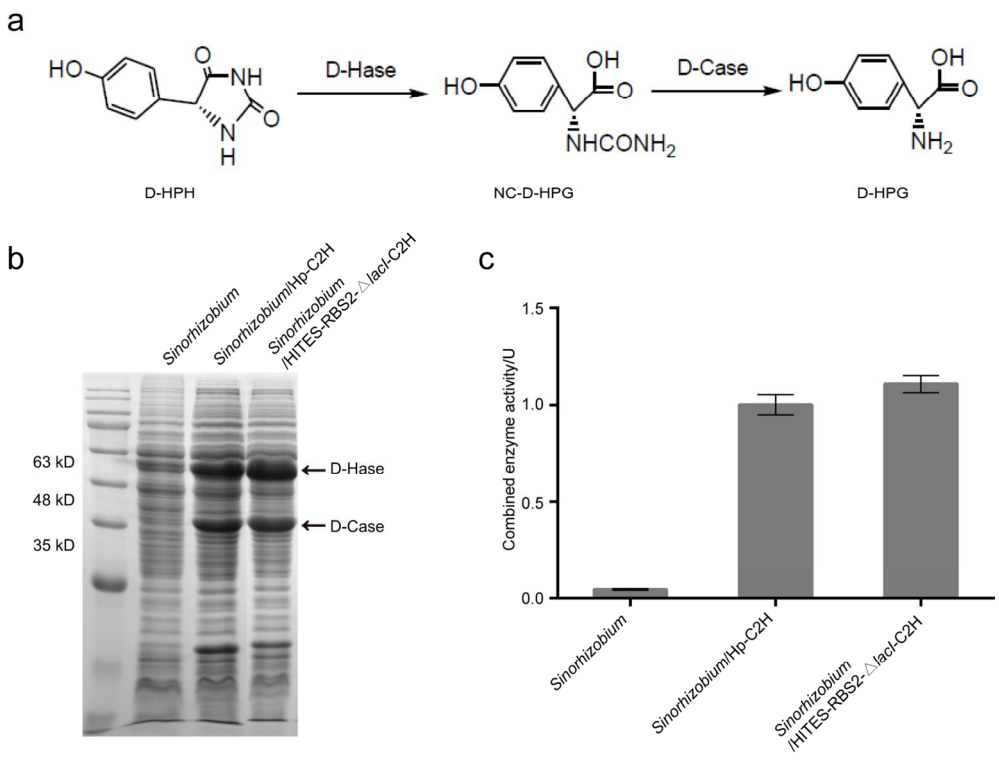

131x99mm (300 x 300 DPI)

Integrating T7 RNA polymerase and its cognate transcriptional units for a host-independent and stable expression system in single plasmid

Xiao Liang, Chenmeng Li, Wenya Wang, Qiang Li

Table of Contents Graphic

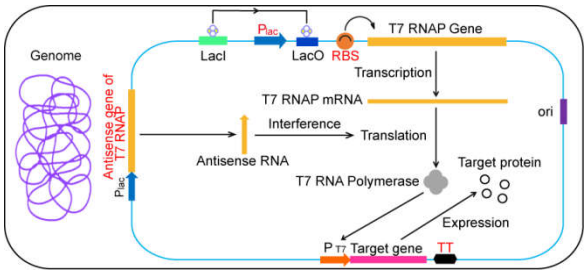

This page is for Table of Contents use only.